

See discussions, stats, and author profiles for this publication at: <https://www.researchgate.net/publication/23799348>

# Enthalpy Difference between Conformations of Normal Alkanes: Raman Spectroscopy Study of n-Pentane and n-Butane

Article in The Journal of Physical Chemistry A · February 2009

DOI: 10.1021/jp809639s · Source: PubMed

CITATIONS

98

READS

1,270

1 author:



Roman Balabin

ETH Zurich

93 PUBLICATIONS 5,278 CITATIONS

SEE PROFILE

# Enthalpy Difference between Conformations of Normal Alkanes: Raman Spectroscopy Study of *n*-Pentane and *n*-Butane

Roman M. Balabin\*

Department of Chemistry and Applied Biosciences, ETH Zurich, 8093 Zurich, Switzerland

Received: July 15, 2008; Revised Manuscript Received: December 2, 2008

Conformation equilibrium in normal pentane ( $C_5H_{12}$ ) was studied by the low-temperature gas-phase Raman spectroscopy method. A special retroreflecting multipass cell was constructed. Gas-phase (vapor) spectra were recorded in the temperature region of  $-130.3$  to  $-23.1$  °C and in the spectral range below  $500\text{ cm}^{-1}$ . The peaks of *trans-trans* ( $399.0\text{ cm}^{-1}$ ), *trans-gauche* ( $328.9\text{ cm}^{-1}$ ), and *gauche(+)-gauche(+)* ( $267.1\text{ cm}^{-1}$ ) conformers (rotamers) of *n*-pentane were assigned using quantum chemistry data (MP2 and B3LYP methods with aug-cc-pVTZ basis set). The contour of each line was deconvoluted using *ab initio* data to obtain precise total integral intensity. The intensities at different temperatures were used to evaluate the enthalpy (energy) difference between *trans-gauche* and *trans-trans* ( $\Delta H_{tg} = 618 \pm 6\text{ cal/mol}$ ), and *gauche(+)-gauche(+)* and *trans-trans* ( $\Delta H_{g+g+} = 940 \pm 20\text{ cal/mol}$ ) conformers. Normal butane (*n*-butane) measurements under similar experimental conditions have been taken to understand the chain length influence. The  $C_4H_{10}$  enthalpy difference value has been evaluated ( $\Delta H_g = 660 \pm 22\text{ cal/mol}$ ). The results are compared with published experimental and theoretical data. The data presented here can be used as a reference for quantum chemistry calculations of conformation equilibrium in *n*-butane and *n*-pentane.

## 1. Introduction

It is a well-known fact that hydrocarbon chains are among the most important structural units in organic chemistry.<sup>1</sup> Information about rotational isomerism, which is possible in chains longer than four carbon atoms, is of great interest to chemists in different research areas. Relative concentrations of different conformations of organic molecules are theoretically and practically important. The influence of conformation equilibrium on intermolecular interaction, solvation,<sup>2,3</sup> and biological activity has been recently recognized.<sup>4,5</sup>

Normal alkanes can be regarded as a simple model for chain molecules, and on the basis of this a great amount of work has been done to evaluate the enthalpy difference between *gauche* (torsion angle of  $60^\circ$ , local minima) and *trans* ( $180^\circ$ , global minima) conformers.

*n*-Butane ( $C_4H_{10}$ ) is the simplest normal hydrocarbon in which conformation equilibrium is possible. After the pioneering work of Pitzer,<sup>6</sup> extensive research has been done on the *trans/gauche* enthalpy difference of *n*-butane in the gas or liquid phases and in solution.<sup>7</sup> A number of methods (including NMR,<sup>8</sup> ultrasonic relaxation,<sup>9</sup> and electron diffraction<sup>10–13</sup>) have been applied for determining relative conformer abundance at various temperatures.

Significantly, only a part of these studies has been conducted in the gas (free<sup>1,14</sup>) phase. However, it is still not clear how conformation stability varies with phase changes. It is claimed<sup>15</sup> that stability of a *gauche* conformer can increase at  $54 \pm 17\text{ cal/mol}$  in liquid phase. This value is in good agreement with experimental data.<sup>16</sup> The solid phase is believed to consist only of molecules in *trans* conformation.<sup>17</sup>

IR and Raman spectroscopy measurements have played an important role in understanding the potential that governs the normal butane conformation equilibrium.<sup>16,18–23</sup> The complexity

of *n*-butane Raman and far-IR spectrum has led to many contradictions in spectra analysis and thermodynamic conclusions (refs 16, 19–21 and refs 18, 23). This shows that nowadays only the first digit in the enthalpy difference ( $670 \pm 100\text{ cal/mol}$  or  $\pm 15\%$ ) between *gauche* and *trans n*-butane conformers is known. This, of course, is not enough for predicting precise properties: For example, the ratio of *trans/gauche* conformers concentration at room temperature can be predicted only with an error of approximately 40%.

Prompted by continuing experimental difficulties in pinpointing the key features of the butane torsion potential, increasingly sophisticated *ab initio* theoretical methods have also been applied to this problem over the last three decades (refs 7, 24 and references therein). It should be noted that evaluation of energy difference below  $<1\text{ kcal/mol}$  is a sophisticated task for modern quantum chemistry.<sup>25</sup> The size of  $C_nH_{2n+2}$  molecule ( $n > 3$ ) makes the evaluation even more difficult.

One should not forget that *n*-butane is just the simplest case; with this, only two conformations are possible but this number increases rapidly and reaches hundreds for *n*-decane ( $C_{10}H_{22}$ ).

The next compound in the row of linear hydrocarbons is normal pentane ( $C_5H_{12}$ ). Four conformations are possible in the case of *n*-pentane (one of them is believed to be sterically forbidden<sup>24</sup>). Owing to the impact of the conformation on orbital energies,<sup>26,27</sup> electron density distributions,<sup>27</sup> and molecular vibrations,<sup>28–31</sup> determining the conformational energies of *n*-pentane<sup>24</sup> has become a mandatory step for a sound interpretation of its ionization,<sup>26</sup> electron momentum,<sup>27</sup> and IR and Raman spectra.<sup>28</sup>

Although many methods were applied, not much precise data could be obtained so far. The situation is more or less similar to that of *n*-butane: Only the first digit in the enthalpy difference between *trans-gauche* and *trans-trans n*-pentane conformers ( $\Delta H_{tg} = 0.60 \pm 0.10\text{ kcal/mol}$ ) is known. No experimental information about relative stability of *gauche(+)-gauche(+)*

\* To whom correspondence should be addressed: Tel.: +41-44-632-4783. E-mail: balabin@org.chem.ethz.ch. On leave from Gubkin Russian State University, Moscow, Russia.

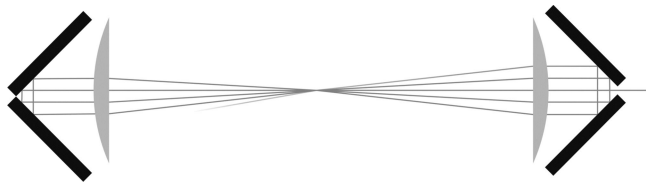


**Figure 1.** A scheme of a retroreflecting multipass cell for low-temperature Raman spectroscopy: mirrors (black), lenses (gray). The laser beam is shown with a gray gradient line.

conformer ( $\Delta H_{g+g+}$ ) is available. The question of additivity<sup>1</sup> of the *gauche-trans* energy difference:  $\Delta H_{g+g+} = 2 \times \Delta H_{tg}$  (?), is still open.

In this study, it was attempted to evaluate the difference in enthalpy between *trans-gauche* and *trans-trans*, and *gauche(+)-gauche(+)* and *trans-trans* conformers of normal pentane using low-temperature gas-phase Raman spectroscopy. The aim of the study was to get a precise value of enthalpy difference between *trans-gauche* and *trans-trans* conformers and to check its additivity in *gauche(+)-gauche(+)* case.

## 2. Experimental Section

**2.1. Raman Setup.** A 457 nm CW diode-pumped solid state (DPSS) laser, with an output power of 4.1 W and a spectral line width of less than 0.1 nm, was used. The average laser power instability was 8% (for a 6 h period). The laser beam diameter was 1.5 mm.

The laser beam was split into two unequal components with an intensity ratio of approximately 99/1 using partial reflectance plate beamsplitter (beam sampler, 45° geometry). Approximately 1% of the laser power was sent to a laser power meter equipped with a high-sensitivity thermopile sensor (15  $\mu$ W power resolution). The result of power measurement was integrated over time with spectra (background) measurement and used for spectra (background) normalization. The remaining 99% of the beam power was sent to the gas-phase cell.

A low-temperature retroreflecting multipass cell for Raman spectroscopy was constructed according to ref 32 (Figure 1). In brief, a cell was constructed using two planoconvex lenses ( $\Phi = 105$  mm,  $f = 400$  mm) with each surface dielectric coated for 99.85% transmission at  $\lambda = 457$  nm. The retroreflecting mirrors (75  $\times$  30 mm) were coated for 99.85% reflectivity ( $\lambda = 457$  nm) at an angle of 45° and polarization perpendicular to the plane containing the incident and reflected light. The cell was constructed for 67 passes. The size of the focal volume of the cell was 0.4  $\times$  1.1 mm ("the width of the focus in a direction out of the plane containing the beams"  $\times$  "the depth of the focus in the plane containing the beams").<sup>32</sup> The gain of the cell was found to be  $48.3 \pm 0.8$  when compared to the one-pass variant (according to nitrogen, *n*-pentane, and *n*-heptane measurements).

The scattered light was collected by an achromatic planoconvex lens ( $\Phi = 50$  mm,  $f = 60$  mm) using 90° geometry. To intensify the signal, the light scattered over 270° angle (opposite direction) was reflected by a spherical mirror through the scattering center onto the collecting lens and a gain of  $\sim 1.8$  was achieved.

The collected light was focused on the entrance slit of a triple spectrometer working in a subtractive mode. Highly effective (2400 gr/mm) diffraction gratings were used at all stages. The Raman photons were detected using a back-illuminated 2048  $\times$  512 pixel 16 bit CCD camera with a pixel size of 13.5  $\times$  13.5  $\mu$ m. The camera was cooled with liquid nitrogen (LN). The quantum efficiency (QE) of the camera was  $\sim 85\%$  in the 400–500 nm region with a maximum at 448 nm. To prevent

spectra contamination by cosmic rays (below), a lead box with 15 cm walls (from top and three sides) was constructed around the CCD camera.

A mercury lamp was used for wavenumber ( $x$  axis) calibration, and pure nitrogen for Raman intensity ( $y$  axis) calibration.

The LN cooling system enabled attaining the cell temperature of  $-190$  °C (83 K) with an accuracy of  $\pm 0.02$  °C (standard deviation at  $-150$  °C for a 4 hour period). A light gas flow (approximately 1 m/s) was organized inside the cell.

The whole setup was placed in a dust-free environmental control chamber with a temperature of  $12 \pm 0.3$  °C and a relative humidity of  $7 \pm 2\%$ . The setup was extremely sensitive to dust and contamination of optical elements.

### 2.2. Experimental Parameters.

***n*-Pentane.** The temperature range from  $-130.3$  to  $-23.1$  °C (142.9 – 250 K) was scanned with a step of  $5.4 \pm 1.8$  °C. The same range in the 1000/T scale is 7–3 K<sup>–1</sup> with an exact step of 0.15 K<sup>–1</sup> (21 points). The minimal temperature was determined by getting a Raman scattering signal from *n*-pentane because the vapor pressure of the solid substance at this temperature ( $-130.3$  °C) is lower than 0.1 Pa.<sup>33</sup> In the region below  $-113.1$  °C, the measurement was conducted at the vapor pressure of *n*-pentane; above  $-113.1$  °C, constant pressure of 1.5 Pa was used. The low pressure prevents gas adsorption on metal surfaces and optical components.

***n*-Butane.** The temperature range from  $-139.8$  to  $-77.1$  °C (133.3 – 196.1 K) was scanned with a step of  $3.9 \pm 0.9$  °C. The same range in the 1000/T scale is 7.5–5.1 K<sup>–1</sup> with an exact step of 0.15 K<sup>–1</sup> (17 points).

The split width of spectrometer was set to 50  $\mu$ m (unless otherwise specified in the text). It corresponds to  $\sim 1$  cm<sup>–1</sup> of spectral resolution. Six spectra were collected at each temperature with a 6 day time interval.

**2.3. Materials.** Normal pentane ( $\geq 99\%$  purity, spectrophoto-metric grade) was obtained from Aldrich. It was stored over molecular sieves and distilled freshly. The purity was checked by gas chromatography (GC) and was found to be more than 99.9%. The fresh substance was stored at  $-20$  °C in argon atmosphere for not more than 5 days.

Normal butane ( $\geq 99.98\%$  purity, research grade) was obtained from Matheson Tri-Gas, Inc. and used without further purification.

**2.4. Conformer Nomenclature.** *n*-Pentane conformer (Figure 2) with two torsion angles of 180° is regarded as *trans-trans* or *tt* (part a of Figure 2) and the conformer with one angle of 180° and another of app. 60° as *trans-gauche* or *tg* (part b of Figure 2). Significantly, for one *gauche* conformation per molecule there was no difference between  $+60^\circ$  and  $-60^\circ$ . The *n*-pentane conformation with two angles of approximately 60° and of the same sign is called *gauche(+)-gauche(+)* or  $g^+g^+$  (part c of Figure 2), and the conformer with two angles of approximately 60° and of different signs *gauche(+)-gauche(–)* or  $g^+g^-$  (part d of Figure 2).

The *tt*, *tg*,  $g^+g^+$ , and  $g^+g^-$  conformations are presented in Figure 2. It is found that one of the angles in the last one ( $g^+g^-$ ) is closer to 90° than to 60° because of steric restrictions.<sup>24</sup> A great concentration of the  $g^+g^-$  conformation is not expected in *n*-pentane because of high negative steric effect.<sup>24,34</sup>

**2.5. Enthalpy Difference.** The enthalpy difference is reported relative to *tt* conformation. For example,  $\Delta H_{g+g+}$  means the difference in enthalpy between the  $g^+g^+$  and *tt* pentane conformations. So,  $\Delta H_{tt}$  equals to zero ( $\Delta H_{tt} = 0$ ).

Calories per mole (cal/mol) was used here as the standard unit of enthalpy (energy).

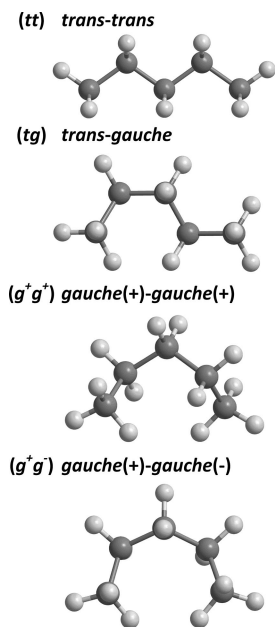


**Figure 2.** Conformations of normal pentane: (tt) *trans-trans* [ $180^\circ$ ,  $180^\circ$ ]; (tg) *trans-gauche* [ $64^\circ$ ,  $176^\circ$ ]; ( $g^+g^+$ ) *gauche(+)-gauche(+)* [ $58^\circ$ ,  $58^\circ$ ]; and ( $g^+g^-$ ) *gauche(+)-gauche(-)* [ $60^\circ$ ,  $-95^\circ$ ]. The values of two dihedral angles are reported in square brackets.

**2.6. Quantum Chemistry Calculations.** Structure optimization of *n*-pentane conformers was done using GAMESS<sup>35</sup> software. Tight self-consistent field (SCF) and optimization criterion was applied for all conformations (except of  $g^+g^+$ ). The second-order Møller–Plesset (MP2)<sup>36,37</sup> and coupled cluster with single and double substitutions with noniterative triple excitation (CCSD(T))<sup>38</sup> levels of theory were applied. Optimization with an analytical gradient is available in MP2 method; numerical optimization was used for CCSD(T) calculations. Two basis sets were used: aug-cc-pVTZ and 6-311++G(d,p).

Geometry of *n*-butane conformers (*trans* and *gauche*) was optimized at MP2/aug-cc-pVTZ and B3LYP/aug-cc-pVTZ levels of theory. No symmetry restrictions were applied.

**2.7. Spectra Deconvolution.** Spectra deconvolution<sup>39</sup> into rotational branches, similar to that in refs 16, 40 was applied. The main difference was the presence of five rotational branches in case of Raman spectrum (O-, P-, Q-, R-, and S-branch).<sup>41</sup> MP2/aug-cc-pVTZ and CCSD(T)/6-311++G(d,p) *n*-pentane conformers were used for obtaining structural parameters. Extra parameters (relative intensities, etc.) were adjusted by robust least-squares procedure<sup>42–44</sup> until the minimal difference with experimental spectra was achieved. No correction for centrifugal distortion was introduced.

**2.8. Software and Computing.** MATLAB computing environment was used for data analysis. Spectra deconvolution using Gaussian-type instrument function was applied (not to be confused with rotational structure deconvolution, above). One hundred and twenty-six ( $126 = 21 \times 6$ ) data points were used for fitting. A self-written program was used for deleting spikes (details below).

**2.9. Inaccuracy.** Unless otherwise specified, the 95% confidence interval is reported as the measure of inaccuracy. As standard deviation is still widely used in literature (even though the probability that the value is within the  $\pm\sigma$  interval is just 68%), its value is sometimes reported for comparison purposes.

### 3. Results and Discussion

#### 3.1. Optimization of Experimental Parameters.

**3.1.1. Cell Parameters Optimization.** The main cell parameter to be optimized was the distance between two lenses (Figure 1) because the total gain (signal intensity) was found to be very sensitive to that distance. A situation similar to that in ref 32 was observed; maximum gain was attained with the lenses positioned closer than the distance determined by the focusing procedure using an autocollimator. The effect was claimed to be the cumulative effect of spherical aberration.<sup>32</sup>

The position and angle of the mirrors and lenses were optimized every 6 h (below).

**3.1.2. Temperature Accuracy.** The accuracy of temperature measurement is important for measuring thermodynamic values. The Raman measurement enables measurement of the real temperature of the sample by comparing the intensities of Stokes and anti-Stokes signals.<sup>45</sup> This technique showed that the sample temperature was maintained at the point set with an accuracy higher than  $0.2^\circ\text{C}$  in a 4 h period in the range from  $-110$  to  $-30^\circ\text{C}$ . This inaccuracy can be acceptable for the purpose of this study.

This accuracy is approximately 20 times better than that of the previous study of *n*-pentane conformations by Raman spectroscopy.<sup>29</sup>

**3.1.3. Time of Measurement.** The optimal time needed for one measurement was worked out by conducting a series of experiments over different durations (0.5, 1.0, 1.5, 2.0, 2.5, 3.0, 4.0, 5.0, 6.0, 7.0, 8.0, and 10 h). The setup stability made it possible to conduct 6 h experiments because after this a small adjustment of the setup was needed to maximize the signal.

The duration for collecting one spectrum was set to 2 h for *n*-pentane vapor pressure of 1.5 Pa (higher than  $-113.1^\circ\text{C}$ ), 3 h for temperature range from  $-123.9$  to  $-116.9^\circ\text{C}$ , and 6 h for temperatures below  $-127.2^\circ\text{C}$ . During this period, 15 sample spectra and 15 background spectra were collected one-by-one (4, 6, or 12 min of accumulation time each). Then 15 background-corrected spectra were obtained by subtraction of a corresponding background spectrum from a sample spectrum (both normalized to integral laser power, Experimental Section). They were averaged in a special way (described below) to get rid of the signal from pixels that have been hit by cosmic rays (below).

The same parameters were used for *n*-C<sub>4</sub>H<sub>10</sub> measurements.

**3.1.4. Cosmic Rays.** The cosmic radiation hitting the CCD chip is a well-known problem both in astronomy and spectroscopy.<sup>46</sup> There are two ways of controlling the effect of cosmic rays on the spectra: “physical” (preventing the CCD hitting) and “mathematical” (as the pixels hit are randomly distributed over the entire spectra, they can be distinguished by statistical methods). Both were applied in this study: (1) the CCD camera was protected by 15 cm thick lead cover (above) that resulted in hit pixels reducing by  $\sim 35\%$  (according to background spectrum measurement); (2) an iterative procedure (close to that of Hill and Rogalla<sup>46a</sup>) for spikes deletion and spectra normalization was applied until the difference between two consecutive results (normalized spectra) becomes negligible.

**3.2. Spectra Analysis.** In Figure 3, one can see an example of *n*-pentane Raman spectra in the range  $250\text{--}430\text{ cm}^{-1}$ . Three conformers can easily be distinguished: *tt* conformer with a maximum at  $399.0 \pm 0.2\text{ cm}^{-1}$ , *tg* conformer with a maximum at  $328.9 \pm 0.2\text{ cm}^{-1}$ , and  $g^+g^+$  conformer with a maximum at  $267.1 \pm 0.3\text{ cm}^{-1}$ . Two of them were already reported,<sup>29</sup> whereas the last one is being reported here for the first time.

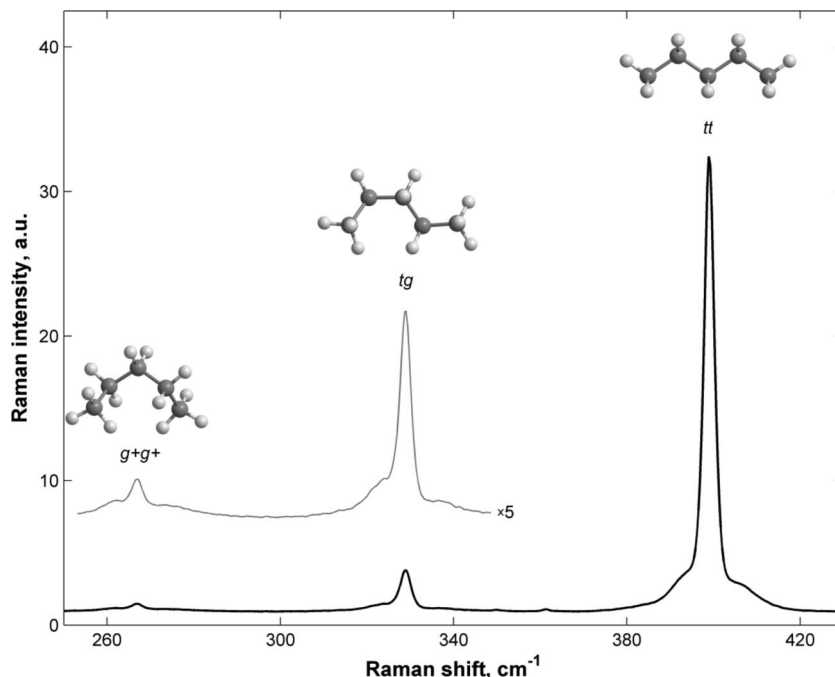


**Figure 3.** Experimental Raman spectra of *n*-pentane (250–430  $\text{cm}^{-1}$ ) in a gas phase at  $-130.3\text{ }^{\circ}\text{C}$ . The spectra are presented after background correction, normalization (to the mean value), and Savitzky–Golay filtering (second-order polynomial, a frame size of seven pixels). The spectrum in the region of 253–348  $\text{cm}^{-1}$  with a magnified intensity ( $\times 5$ ) is also presented. The band assignment: (*tt*) *trans-trans* conformer – 399.0  $\text{cm}^{-1}$ , (*tg*) *trans-gauche* conformer – 328.9  $\text{cm}^{-1}$ , ( $g^{+}g^{+}$ ) *gauche*(+)-*gauche*(+) conformer – 267.1  $\text{cm}^{-1}$ . The ratio of  $g^{+}g^{+}/tt$  and  $tg/tt$  peaks is the lowest in the temperature range studied.

**TABLE 1: Comparison of Experimental and Calculated Raman Active Vibrations (the Most Intense Ones) for *n*-Pentane Conformers in a Frequency Region below 500  $\text{cm}^{-1}$ <sup>a</sup>**

Conformation		Experimental	Calculated			
			<i>ab initio</i>		DFT	
			HF	MP2	SVWN5	B3LYP
<i>trans-trans</i>	<i>tt</i>	$399.0 \pm 0.2$	421.4	402.0	399.2	396.9
<i>trans-gauche</i>	<i>tg</i>	$328.9 \pm 0.2$	349.2	330.4	325.8	327.9
<i>gauche</i> (+)- <i>gauche</i> (+)	$g^{+}g^{+}$	$267.1 \pm 0.3$	282.8	267.9	266.5	268.3
<i>gauche</i> (+)- <i>gauche</i> (-)	$g^{+}g^{-}$	$362\text{ (?)}$ <sup>b</sup>	379.7	363.6	354.9	354.7

<sup>a</sup> Wavenumbers ( $\text{cm}^{-1}$ ) are presented. Basis set: aug-cc-pVTZ (5D 7F) {506 basis functions}; tight self-consistent field (SCF) and optimization conditions (except of  $g^{+}g^{+}$  conformer). No scaling factor has been applied. <sup>b</sup> Too weak signal to be exactly related to  $g^{+}g^{-}$  conformation.

The experimental results (peak positions) are in good agreement with quantum chemistry calculations (Table 1). While Hartree–Fock (HF) and second-order Møller–Plesset perturbation theory (MP2) predictions differ from experiment values by 19.4 and 1.8  $\text{cm}^{-1}$ , respectively, Density functional theory (DFT) predictions (B3LYP and SVWN5 methods) differ by just 1.5 and 1.3  $\text{cm}^{-1}$  (Table 1). It should be noted that with a factor of 0.95 hartree–Fock frequencies differ from experiment by just 1.9  $\text{cm}^{-1}$ .

A weak Raman signal near 362  $\text{cm}^{-1}$  has been observed. It could be attributed to  $g^{+}g^{-}$  conformation. Unfortunately, the signal is too weak to say anything for sure. Its position is close to MP2/aug-cc-pVTZ prediction for  $g^{+}g^{-}$  conformation but rather far from B3LYP/aug-cc-pVTZ results (Table 1). Extra research (in another temperature range) is needed.

The *tt* and *tg* peaks have a similar structure: a sharp peak on a wide basement. This structure can be explained by the presence of five rotational branches: four nonintense wide branches (O-, P-, R-, and S-branch) and one intense sharp branch (Q-branch).<sup>38</sup> The  $g^{+}g^{+}$  peak structure is not intense enough (from 2 to 7% of *tt* intensity depending on a temperature) to show up. All of the peaks are asymmetric,

the main reason being the inequality between the intensities of O- and S-, and P- and R-branches.

For exact evaluation of peak intensity, one needs to deconvolute the total spectral contour into the conformers' contours. For this, the rotational structure of each branch is needed (Experimental Section). Using this technique, it is possible to obtain precise relative intensities even if extra peaks are present in the same region (ref 37 as an example). Even though the integral intensity of O-, P-, R-, and S-branches is less than the intensity of the Q-branch, the influence of these branches should not be neglected in precisely evaluating peak intensities (especially in  $g^{+}g^{+}$  case).

The experimental and predicted rotational structures for the *tt* band (399.0  $\text{cm}^{-1}$ ) are shown in Figure 4. It can be seen that peak deconvolution, as desired, was successfully achieved, implying thereby that evaluation of the peak intensity is much more exact.

### 3.3. Enthalpy Difference: *trans-gauche* (*tg*) Conformation.

Figure 5 depicts the plot of *tt* and *tg* peaks intensities ratio versus reverse thermodynamic temperature. High linearity ( $R^2 = 0.9996$ ) means that the enthalpy difference ( $\Delta H_{tg}$ ) is constant over the entire region of 143–250 K. Using the slope of the

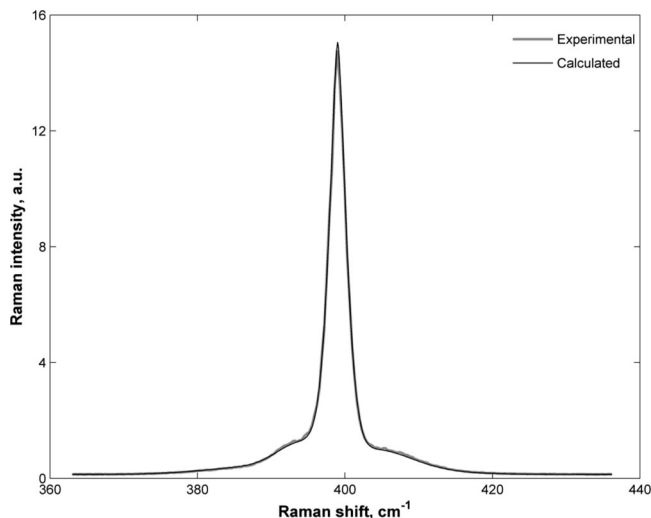


**Figure 4.** Experimental and calculated contours of *trans-trans* (*tt*) *n*-pentane conformer line ( $399.0\text{ cm}^{-1}$ ) in the gas phase at  $-127.2\text{ }^{\circ}\text{C}$ . The intensity is normalized to the mean value. A separate baseline correction is applied.

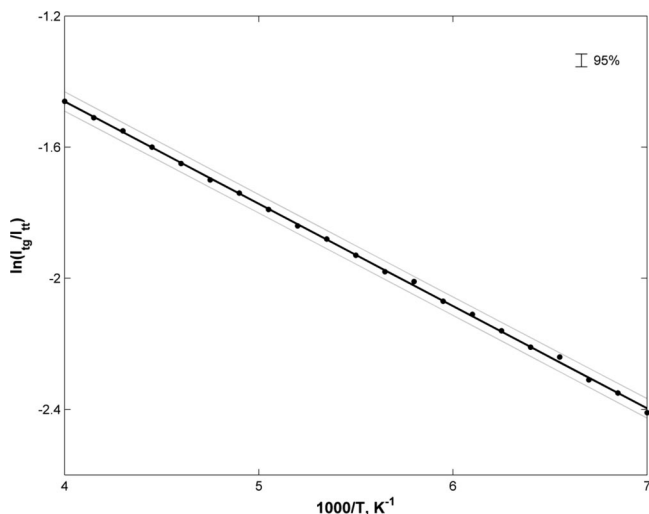


**Figure 5.** Dependence of natural logarithm of peaks integral intensity ratio between *trans-gauche* (*tg*) and *trans-trans* (*tt*) *n*-pentane conformers on the reverse thermodynamic temperature (black circles). The linear fit ( $R^2 = 0.9996$ , black line) is presented with 95% error bounds (gray lines). The mean 95% confidence interval for the experimental points is presented in the right-upper corner. The interval is approximately two times larger for low-temperature points than that for high-temperature ones. Enthalpy difference:  $\Delta H_{tg} = 618 \pm 6\text{ cal/mol}$  ( $216 \pm 2\text{ cm}^{-1}$ ).

line, one can evaluate the enthalpy difference between *trans-gauche* and all-*trans* conformations of normal pentane as  $618 \pm 6\text{ cal/mol}$  (or  $618 \pm 3\text{ cal/mol}$ , if standard deviation is used as an uncertainty value).

**3.4. Enthalpy Difference: *gauche*(+)-*gauche*(+) ( $g^+g^+$ ) conformation.** The dependence of relative intensity of the  $g^+g^+$  peak ( $267.1\text{ cm}^{-1}$ ) is shown in Figure 6. A high linearity, similar to that in Figure 5 for *tg*, is observed ( $R^2 = 0.9973$ ). So, the constant value for  $\Delta H_{g^+g^+}$  is also observed. The enthalpy difference between *gauch*(+)-*gauche*(+) and all-*trans* conformations of normal pentane is  $940 \pm 20\text{ cal/mol}$  (or  $942 \pm 12\text{ cal/mol}$ , if standard deviation is used as an uncertainty value).

**3.5. Comparison with Previously Published Experimental Data.** In this section, the energy values obtained here are compared with published experimental values.

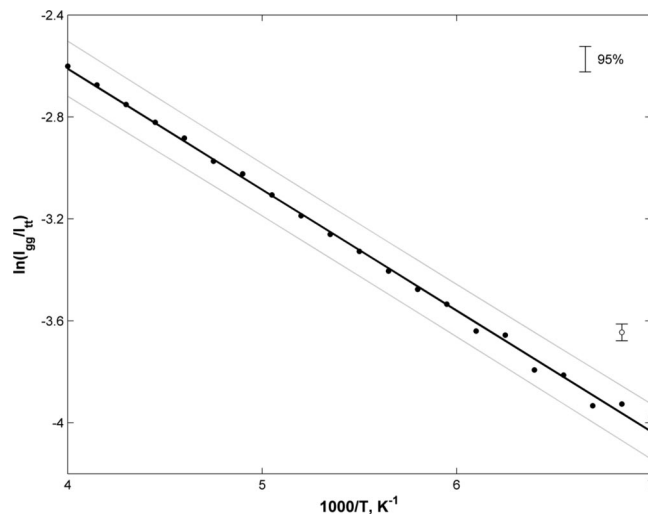


**Figure 6.** Dependence of natural logarithm of peaks integral intensity ratio between *gauche*(+)-*gauche*(+) ( $g^+g^+$ ) and *trans-trans* (*tt*) *n*-pentane conformers on the reverse thermodynamic temperature (black circles). The linear fit ( $R^2 = 0.9973$ , black line) is presented with 95% error bounds (gray lines). The mean 95% confidence interval for the experimental points is presented in the right-upper corner. The interval is approximately three times larger for low-temperature points than that for high-temperature ones. Enthalpy difference:  $\Delta H_{g^+g^+} = 940 \pm 20\text{ cal/mol}$  ( $329 \pm 7\text{ cm}^{-1}$ ). Open circle represents the value of the peaks integral intensity ratio that has been reproduced twice but is still believed to be an experimental error (no further experiments confirmed it).

**3.5.1. *trans-gauche* (*tg*) Conformation.** The value of  $\Delta H_{tg}$  ( $618 \pm 3\text{ cal/mol}$ ) can be compared with that of  $465 \pm 30\text{ cal/mol}$  (standard deviation), reported by Kanesaka et al.<sup>29</sup> It can be observed from a comparison of Figure 5 with Figure 3 in ref 29 that the data presented here are much more exact. There are two possible reasons for this: (i) A temperature range, much lower than the one (260–300 K) in ref 29, or (ii) the temperature accuracy achieved is approximately 20 times more (above). No spectral peak deconvolution was applied in ref 29.

It should also be noted that the recalculation of 95% confidence interval in ref 29 (based on available graphical data) gave a value of  $\pm 72\text{ cal/mol}$ .

So, one can conclude that the experimental value of  $618 \pm 6\text{ cal/mol}$  ( $2.59 \pm 0.02\text{ kJ/mol}$  or  $216 \pm 2\text{ cm}^{-1}$ ) can be used as a reference for enthalpy difference between *tg* and *tt* conformers of *n*-pentane.

**3.5.2. *gauche*(+)-*gauche*(+) ( $g^+g^+$ ) Conformation – Enthalpy Additivity Check.** The author believes that his value of enthalpy difference between *gauch*(+)-*gauche*(+) and all-*trans* conformations is the first experimental value to be published. Even though the uncertainty in this case is 4 times more than that in the case of *tg* conformer, the value of  $940 \pm 20\text{ cal/mol}$  ( $3.93 \pm 0.09\text{ kJ/mol}$  or  $329 \pm 7\text{ cm}^{-1}$ ) can still be used as a reference value for quantum chemistry methods.

It should be noted that enthalpy difference for *n*-pentane conformers is highly nonadditive ( $\Delta H_{g^+g^+} \neq 2\Delta H_{tg}$ ); the difference between observed and additive value ( $2\Delta H_{tg}$ ) is  $-31\%$ . So, one cannot freely assume that each *gauche* conformation has a constant energy cost.<sup>1</sup> One can assume that the major part of the energy lowering in  $g^+g^+$  conformation is due to dispersion interactions.<sup>47</sup> This conclusion is important for molecular dynamic simulations (Section 3.7).

**3.5.3. *n*-Butane.** The experimental value of enthalpy difference for *n*-butane is  $670 \pm 100\text{ cal/mol}$ .<sup>24</sup> From these data, it is hard to say anything about transferability of the enthalpy difference (inside the same class of hydrocarbons). It is not clear

whether the 8% difference between the  $C_4H_{10}$  and  $C_5H_{12}$  values is due to the hydrocarbon size or experimental uncertainty. One needs more exact  $\Delta H_{ig}$  value for *n*-butane to arrive at definite conclusions. However, the value reported in this Raman study is much closer to 670 cal/mol than the one reported previously ( $465 \pm 30$  cal/mol, 31% difference).

Of course, further experimental values for *n*-hexane, *n*-heptane, and so forth are needed to make general conclusions about the whole row of normal alkanes.

**3.6. Experimental Study of *n*-Butane.** To clarify the issue stated in Section 3.5.3, *n*-butane measurements under the same experimental conditions have been carried out. It should be noted that Raman study of *n*-butane is much more sophisticated, because *all* Raman-active vibrations of *trans*-butane conformation overlap with the *gauche* ones (Table 5 in Murphy et al.<sup>48</sup> and Table 8 in Durig et al.<sup>49</sup>). Murphy<sup>50</sup> has already discussed this issue in 1992 (Figures 1 and 2 therein).

Because we are not able to find a well-separated pair of peaks belonging to different *n*-butane conformations, we have used a peak contour to evaluate the conformers' fractions. Such a technique makes it possible to get the values of  $\sim 1\%$  accuracy (maximum), which greatly decreases the quality of enthalpy evaluation.

It was decided to use a pair of peaks at  $430.1\text{ cm}^{-1}$  (*trans*,  $430.0\text{ cm}^{-1}$  according to ref 48) and  $320.5\text{ cm}^{-1}$  (*gauche*,  $319.5\text{ cm}^{-1}$  according to ref 48). However, the *trans* peak is contaminated by IR and Raman-active  $\nu_{35}$  *gauche* vibration at  $430.5\text{ cm}^{-1}$  ( $429.2\text{ cm}^{-1}$  according to refs 48, 51). The ratio of the last two peak intensities ( $I_{430}/I_{g,431}$ ) is predicted (MP2/6-311+G\*) to be 13.1; so the intensity of *gauche* vibration is more than an order of magnitude lower than that of the *trans* one. Since *n*-butane *gauche* fraction in this temperature range is  $\sim 10\%$ , contamination of the *trans* vibration is  $\sim 10^{-2}$ . It should be noted that  $\nu_{35}$  *trans*-butane frequency ( $430.1\text{ cm}^{-1}$ ) is the best choice because all other *trans* vibrations are more contaminated (greater  $I_g/I_t$  ratio). Existence of  $431\text{ cm}^{-1}$  *gauche* vibration prevents us from going to higher temperature regions (as has been done for *n*-pentane).

Figure 7 presents the results of our experimental study of *n*- $C_4H_{10}$ . The enthalpy difference between *gauche* and *trans* conformations of *n*-butane was found to be  $660 \pm 22$  cal/mol (95%). The reason for 3.6 times greater uncertainty is the neglect of  $431\text{ cm}^{-1}$  (*gauche*) peak influence on the  $I_g/I_t$  intensity ratio. Without compensating for this effect, one should not expect better accuracy. Anyway, our value is 4.6 times more accurate than that previously reported ( $670 \pm 100$  cal/mol, above) and much closer to other experimental values than the earlier Raman studies ( $1089 \pm 117$  and  $1055 \pm 206$  cal/mol,<sup>48</sup> using van't Hoff plot), and  $690 \pm 100$  cal/mol<sup>49</sup> (by neglect of the entropy difference:  $\Delta S_g = 0$ ).

The comparison of  $C_4$  ( $660 \pm 22$  cal/mol) and  $C_5$  ( $618 \pm 6$  cal/mol) values of enthalpy difference (for one *gauche* angle) leads to a conclusion of the decrease in energy difference with chain length increase. Even though the decrease is rather small ( $42 \pm 28$  cal/mol or  $6 \pm 4\%$ ), it can greatly influence higher normal alkanes ( $C_8$ – $C_{20}$ ) if the same size-dependence is valid there. Further experimental research for *n*-alkanes (*n*-hexane, *n*-heptane, etc.) is needed to clarify this issue.

It seems that even though *n*-butane is the simplest hydrocarbon for which conformation equilibrium is possible, it is one of the worst substances for Raman spectroscopy study. The fact that no contamination-free vibrations of *trans* conformer are

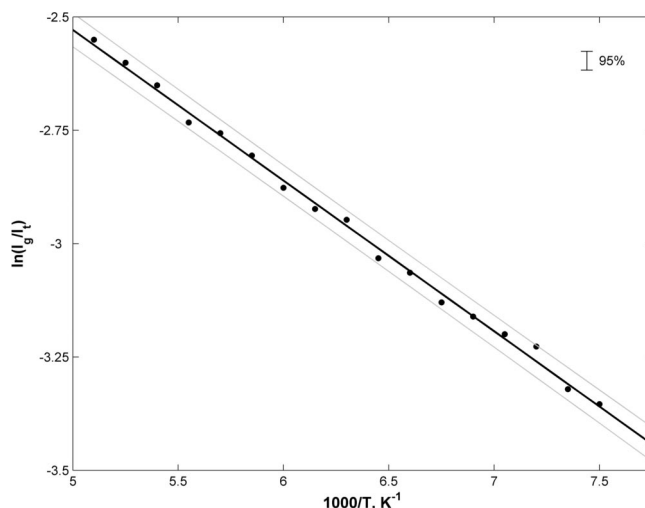


**Figure 7.** Dependence of natural logarithm of peaks integral intensity ratio between *gauche* (*g*) and *trans* (*t*) *n*-butane conformers on the reverse thermodynamic temperature (black circles). The linear fit ( $R^2 = 0.9964$ , black line) is presented with 95% error bounds (gray lines). The mean 95% confidence interval for the experimental points is presented in the right-upper corner. The interval is approximately two times larger for low-temperature points than that for high-temperature ones. Enthalpy difference:  $\Delta H_{ig} = 660 \pm 22$  cal/mol ( $231 \pm 8\text{ cm}^{-1}$ ).

Raman active leads to great problems for data analysis (ref 50 for further discussion).

### 3.7. Comparison with Previously Published *ab initio* Data.

In this section, the values obtained here are compared with published calculated values. Only *ab initio* values are considered; the values of DFT methods are considerably higher<sup>24</sup> (because dispersion interactions are not considered by standard DFT functionals<sup>52</sup>).

Enthalpy difference should be distinguished from electronic energy difference (standard value reported for calculations).<sup>24</sup> The influence of zero-point energy (ZPE) and thermal correction cannot be neglected when accuracy higher than 100 cal/mol is necessary.<sup>24</sup> For both of these corrections, structure optimization and vibrational analysis are needed.

In ref 53, the energy (not enthalpy) difference between *n*-pentane conformers was evaluated using the MP2/6-31G\* level of theory, and values of 670 and 1090 cal/mol were reported for *tg* and  $g^+g^+$  conformations. The difference between these values and experimental enthalpies are 8 and 16% for *tg* and  $g^+g^+$  conformations, respectively.

A focal point analysis for different *n*-pentane conformers (up to 635 basis functions), including CCSD(T) level, was attempted by Salam and Deleuze,<sup>24</sup> who reported 621 and 1065 cal/mol for *tg* and  $g^+g^+$  conformations. The fact that these values differ from experimental *tg* and  $g^+g^+$  values by just 0.5 and 13% respectively can be explained as due to an error compensation because the addition of ZPE correction<sup>24</sup> leads to a difference of 9 and 51%, respectively.

It should be noted that nowadays (mid-2008) application of CCSD(T) level of theory with at least medium size basis set (e.g., aug-cc-pVTZ<sup>54</sup>) for structure optimization and frequency calculation of *n*-pentane molecule is not possible. No composite method (e.g. reported by Salam and Deleuze<sup>24</sup> where molecular structures of four conformers were optimized at the B3LYP/6-311++G\*\* level) seems to be reliable enough.

Even though quantum chemistry methods have greatly helped this research by vibrational (Table 1) and rotational analysis

(Figure 4), their reliability in energy (or enthalpy) predictions is still doubtful. More reliably, ab initio data is expected in the next 5–10 years.

The present experimental data confirm the idea of Klauda et al.<sup>55</sup> and Salam and Deleuze<sup>24</sup> regarding nonadditivity of adjacent *gauche* state energies in normal alkanes. The fact that attractive methylmethyl interactions stabilize  $g^+g^+$  conformation is confirmed by experiment. The magnitude of such a stabilization is found to be  $290 \pm 30$  cal/mol, which is not far from 177 cal/mol reported by Salam and Deleuze<sup>24</sup> for  $2 \times \Delta E_{g^+g^+} - \Delta E_{ig}$ . One should note that the sign of the ab initio ZPE-corrected  $\Delta(\Delta E)$  value is different ( $-72$  cal/mol).<sup>24</sup> See references within refs 24, 55 for further discussion.

Note that the energy lowering in the  $g^+g^+$  conformation was first studied in 1991 by Tsuzuki et al.<sup>56</sup> using ab initio calculations [MP4(SDQ)/6-31G\*\*/6-31G\*]. They concluded that the dispersion interaction is the cause of energy lowering ( $\sim 160$  cal/mol).

All presented calculations have not been corrected for intramolecular basis set superposition error (BSSE).<sup>57</sup>

#### 4. Conclusions

The following conclusions are drawn:

1. The enthalpy difference between *n*-pentane conformations is found to be  $618 \pm 6$  and  $940 \pm 20$  cal/mol for *trans-gauche* and *trans-trans*, and *gauche(+)-gauche(+)* and *trans-trans*, respectively.

2. The nonadditivity ( $-31\%$ ) of enthalpy difference is shown. An effect of energy lowering due to dispersion interactions<sup>58–60</sup> is experimentally evaluated.

3. The enthalpy difference between *trans* and *gauche* conformations of *n*-butane is found to be  $660 \pm 22$  cal/mol or  $42 \pm 28$  cal/mol ( $6 \pm 4\%$ ) higher than that of *n*-pentane.<sup>59</sup>

4. The major Raman active vibrations of *n*-pentane conformers in the spectral range below  $500\text{ cm}^{-1}$  are at  $399.0 \pm 0.2$ ,  $328.9 \pm 0.2$ , and  $267.1 \pm 0.3\text{ cm}^{-1}$  for *trans-trans*, *trans-gauche* and *gauche(+)-gauche(+)*, respectively.

5. A signal from the *gauche(+)-gauche(-)* conformation (probably?) has been observed. A high negative steric effect for this conformation has been confirmed. Extra research is needed to confirm these data.

**Acknowledgment.** The author thanks Prof. Dr. M. Suhm for the opportunity given to familiarize himself with the jet-cooled Raman setup as a part of Graduate School (GRK 782) studies in the Georg-August University of Göttingen. Support by the German Research Foundation (DFG) is acknowledged. The components for Raman setup have been manufactured by the Federal State Unitary Enterprise Research Center “Vavilov State Optical Institute”. The assistance of Saint-Petersburg State University of Information Technologies, Mechanics and Optics (Saint-Petersburg, Russia) and Ministry of Defence of the Russian Federation is acknowledged. A. Borisov is acknowledged for technical assistance; I. Samoilenko is acknowledged for computational assistance (software and hardware). The author is grateful to the Government of Russian Federation for a special (nominative) scholarship and to the ITERA International Group of companies for a scholarship.

#### References and Notes

- (1) Bartell, L. S.; Kohl, D. A. *J. Chem. Phys.* **1963**, *39*, 3097.
- (2) Hirata, F. *Molecular Theory of Solvation*; Springer: New York, 2003.
- (3) Baldwin, R.; Baker, D. *Peptide Solvation and H-bonds*; Academic Press: New York, 2006.
- (4) Srinivasan, R.; Sarma, R. H. *Conformation in Biology*; Adenine Press: New York, 1982.
- (5) Lodish, H.; Berk, A.; Kaiser, C. A.; Krieger, M.; Scott, M. P.; Bretscher, A.; Ploegh, H.; Matsudaira, P. T. *Molecular Cell Biology*; W.H. Freeman & Co Ltd: New York, 2007.
- (6) Pitzer, K. S. *J. Chem. Phys.* **1940**, *8*, 711.
- (7) Allinger, N. L.; Fermann, J. T.; Allen, W. D.; Schaefer, H. F. *J. Chem. Phys.* **1997**, *106*, 5143.
- (8) Woller, P. B.; Garbisch, E. W., Jr. *J. Am. Chem. Soc.* **1972**, *94*, 5310.
- (9) Piercy, J. E.; Rao, M. G. S. *J. Chem. Phys.* **1967**, *46*, 3951.
- (10) Bonham, R. A.; Bartell, L. S. *J. Am. Chem. Soc.* **1959**, *81*, 3491.
- (11) Bartell, L. S.; Kohl, D. A. *J. Chem. Phys.* **1963**, *39*, 3097.
- (12) Bradford, W. F.; Fitzwater, S.; Bartell, L. S. *J. Mol. Struct.* **1977**, *38*, 185.
- (13) Heenan, R. K.; Bartell, L. S. *J. Chem. Phys.* **1983**, *78*, 1270.
- (14) Freund, S. M.; Maier, N. B.; Holland, F. R.; Beattie, W. H. *J. Chem. Phys.* **1978**, *69*, 1961.
- (15) DeVaure, J.; Lascombe, J. *Nouv. J. Chim.* **1979**, *3*, 579.
- (16) Herrebout, W. A.; van der Veken, B. J.; Wang, A.; Durig, J. R. *J. Phys. Chem.* **1995**, *99*, 578.
- (17) Schaufele, R. F.; Shimanouchi, T. *J. Chem. Phys.* **1967**, *47*, 3605.
- (18) Compton, D. A. C.; Montero, S.; Murphy, W. F. *J. Chem. Phys.* **1980**, *84*, 3587.
- (19) Durig, J. R.; Compton, D. A. C. *J. Phys. Chem.* **1979**, *83*, 265.
- (20) Stidham, H. D.; Durig, J. R. *Spectrochim. Acta, Part A* **1986**, *42*, 105.
- (21) Durig, J. R.; Wang, A.; Beshir, W.; Little, T. S. *J. Raman Spectrosc.* **1991**, *22*, 683.
- (22) Golebiewski, A.; Parczewski, A. *Chem. Rev.* **1974**, *74*, 519.
- (23) Murphy, W. F.; Fernandez-Sanchez, J. M.; Raghavachari, K. *J. Phys. Chem.* **1991**, *95*, 1124.
- (24) Salam, A.; Deleuze, M. S. *J. Chem. Phys.* **2002**, *116*, 1296.
- (25) Bartlett, R. J. *J. Phys. Chem.* **1989**, *93*, 1697.
- (26) Deleuze, M.; Delhalle, J.; Pickup, B. T.; Svensson, S. *J. Am. Chem. Soc.* **1994**, *116*, 10715.
- (27) Deleuze, M. S.; Pang, W.; Salam, A.; Shang, R. C. *J. Am. Chem. Soc.* **2001**, *123*, 4049.
- (28) Gough, K. M.; Srivastava, H. K. *J. Phys. Chem.* **1996**, *100*, 5210.
- (29) Kanesaka, I.; Snyder, R. G.; Strauss, H. L. *J. Chem. Phys.* **1986**, *84*, 395.
- (30) Snyder, R. G. *J. Chem. Phys.* **1967**, *47*, 1316.
- (31) Sheppard, N.; Szasz, G. J. *J. Chem. Phys.* **1949**, *17*, 86.
- (32) Hill, R. A.; Mulac, A. J.; Hackett, C. E. *Appl. Opt.* **1977**, *16*, 2044.
- (33) Ruzicka, K.; Majer, V. *J. Phys. Chem. Ref. Data* **1994**, *23*, 1.
- (34) Klauda, J. B.; Brooks, B. R.; MacKerell, A. D.; Venable, R. M.; Pastor, R. W. *J. Phys. Chem. B* **2005**, *109*, 5300.
- (35) Schmidt, M. W.; Baldridge, K. K.; Boatz, J. A.; Elbert, S. T.; Gordon, M. S.; Jensen, J. H.; Koseki, S.; Matsunaga, N.; Nguyen, K. A.; Su, S. J.; Windus, T. L.; Dupuis, M.; Montgomery, J. A. *J. Comput. Chem.* **1993**, *14*, 1347.
- (36) Möller, C.; Plesset, M. S. *Phys. Rev.* **1934**, *46*, 618.
- (37) Head-Gordon, M.; Pople, J. A.; Frisch, J. M. *Chem. Phys. Lett.* **1988**, *153*, 503.
- (38) Pople, J. A.; Head-Gordon, M.; Raghavachari, K. *J. Chem. Phys.* **1987**, *87*, 5968.
- (39) Western, C. M. *PGOPHER, A Program for Simulating Rotational Structure*; University of Bristol. <http://pgopher.chm.bris.ac.uk>.
- (40) Pistorius, A. M. A.; DeGrip, W. J. *Vib. Spectrosc.* **2004**, *36*, 89.
- (41) Herzberg, G. *Molecular Spectra and Molecular Structure: Infrared and Raman of Polyatomic Molecules*; Krieger Pub Co: Malabar, FL, 1991.
- (42) Maronna, R. A.; Martin, D. R.; Yohai, V. J. *Robust Statistics: Theory and Methods*; Wiley: New York, 2006.
- (43) Balabin, R. M.; Safieva, R. Z.; Lomakina, E. I. *Chemometr. Intell. Lab. Syst.* **2008**, *93*, 58.
- (44) Balabin, R. M.; Safieva, R. Z.; Lomakina, E. I. *Chemometr. Intell. Lab. Syst.* **2007**, *88*, 183.
- (45) Goldbrunner, M.; Karl, J.; Hein, D. *Kerntechnik* **2003**, *68*, 106.
- (46) (a) Hill, W.; Rogalla, D. *Anal. Chem.* **1992**, *64*, 2575. (b) Groom, D. *Exp. Astron.* **2002**, *14*, 45.
- (47) Suhm, M. Private communication, 2007.
- (48) Murphy, W. F.; Fernandez-Sanchez, J. M.; Raghavachari, K. *J. Phys. Chem.* **1991**, *95*, 1124.
- (49) Durig, J. R.; Wang, A.; Beshir, W.; Little, T. S. *J. Raman Spec.* **1991**, *22*, 683.
- (50) Murphy, W. F. *J. Raman Spec.* **1992**, *23*, 413.
- (51) Stidham, H. D.; Durig, J. R. *Spectrochim. Acta* **1986**, *42A*, 105.
- (52) Grimme, S. Private communication, 2008.

- (53) Mirkin, N. G.; Krimm, S. *J. Phys. Chem.* **1993**, 97, 13887.  
(54) Dunning, T. H. *J. Phys. Chem. A* **2000**, 104, 9062.  
(55) Klauda, J. B.; Brooks, B. R.; MacKerell, A. D.; Venable, R. M.; Pastor, R. W. *J. Phys. Chem. B* **2005**, 109, 5300.  
(56) Tsuzuki, S.; Schafer, L.; Goto, H.; Jemmis, E. D.; Hosoya, H.; Siam, K.; Tanabe, K.; Osawa, E. *J. Am. Chem. Soc.* **1991**, 113, 4665.  
(57) Balabin, R. M. *J. Chem. Phys.* **2008**, 129, 164101.  
(58) Balabin, R. M.; Syunyaev, R. Z.; Karpov, S. A. *Energy Fuels* **2007**, 21, 2460.  
(59) Balabin, R. M.; Syunyaev, R. Z. *J. Colloid Interface Sci.* **2008**, 318, 167.  
(60) Balabin, R. M. *Chem. Phys.* **2008**, 352, 267.

JP809639S